ISSN 1062-8738, Bulletin of the Russian Academy of Sciences: Physics, 2023, Vol. 87, No. 7, pp. 910–914. © Allerton Press, Inc., 2023.
Russian Text © The Author(s), 2023, published in Izvestiya Rossiiskoi Akademii Nauk, Seriya Fizicheskaya, 2023, Vol. 87, No. 7, pp. 973–978.

Multicomponent Studies of Extensive Air Showers at Facilities of the NEVOD Experimental Complex

M. B. Amelchakov[a], A. G. Bogdanov[a], D. M. Gromushkin[a], A. N. Dmitrieva[a], R. P. Kokoulin[a], A. Yu. Konovalova[a], K. R. Nugaeva[a], A. A. Petrukhin[a], A. D. Pochestnev[a], S. S. Khokhlov[a, *], I. A. Shulzhenko[a], and E. A. Yuzhakova[a]

[a] *National Research Nuclear University MEPhI, Moscow, 115409 Russia*

**e-mail: sskhokhlov@mephi.ru*

Received December 25, 2022; revised February 12, 2023; accepted March 29, 2023

Abstract—Parameters of extensive air showers detected by the facilities of the NEVOD Experimental Complex are analyzed and compared with events simulated. The calibration and energy threshold of the NEVOD-EAS detector are discussed, as well as the results of retrieval of the axis directions from the NEVOD-EAS and DECOR data. An example of the event detected by all facilities of the complex is given.

DOI: 10.3103/S1062873823702684

INTRODUCTION

Earlier studies of extensive air showers (EASes) revealed a number of unusual phenomena in the interactions of high and ultrahigh energy particles: the measured cosmic ray energy spectrum is of a sharply falling power-law character with a knee in the region of around 5 PeV; the second knee and an excess of multi-muon events relative to all existing models are observed at energies above 100 PeV (the so-called "muon puzzle"). In many experiments, unusual events and phenomena have been observed at energies above 10 PeV (e.g., alignment, penetrating cascades, "Centauros", "anti-Centauros" and halos).

There is currently no generally accepted model that can explain these phenomena within a unified approach. Results from multicomponent studies of EASes in which different components are detected in the same event by different types of detectors can become a key to explaining them. Different experiments (e.g., TAIGA [1] in Russia and LHAASO [2] in China) are headed in this direction.

A complementary approach to analyzing experimental data would appear to be promising in the multicomponent studies of EASes. In this approach, information about one or several shower components that is unimportant in the context of independent analysis can be added to data on other components. This allows more accurate estimates of the parameters of an EAS and thus the particle that initiated it.

Studies using this approach are performed at the NEVOD experimental complex of MEPhI.

NEVOD EXPERIMENTAL COMPLEX

The NEVOD experimental complex combines nine scientific facilities [3]. In this work, we analyze data from six of them: CWC, SCT, DECOR, NEVOD-EAS, PRISMA, and URAN.

Some facilities of the experimental complex are housed inside a building, e.g., the NEVOD Cherenkov water calorimeter (CWC) [4] with a volume of 2000 m^3 and a spatial lattice of 91 quasi-spherical modules inside. The CWC measures the energy released by charged particles. The planes of the scintillation detectors of the system of calibration telescopes are on the bottom and the cover of the CWC [5]. Each plane contains 40 detectors, allowing us to calibrate the CWC's PMTs and study the electron–photon and muon EAS components in the 10^{14}–10^{17} eV range of energies. The DECOR coordinate detector is mounted around the CWC. It consists of eight vertical supermodules with a total area of 70 m^2 [6]. DECOR allows us to detect groups of muons in inclined EASes and analyze the density of particles in these groups.

The NEVOD-EAS facility is positioned around the NEVOD Experimental Complex on the roofs of buildings and the adjacent territory [7]. It consists of nine clusters, each of which has four detector stations. The total area of the facility is 10^4 m^2. NEVOD-EAS allows us to obtain EAS parameters in a classical way (i.e., from the electron–photon component).

The PRISMA facility is located on the fourth floor of the building of the NEVOD Experimental Complex. It consists of two clusters of 16 electron–neutron detectors each [8] and occupies an area of 500 m^2. PRISMA allows us to detect the electron–photon

component [9] and EAS thermal neutrons produced by interactions of the hadron component of EAS with the matter surrounding the detector.

The URAN facility is the next step in detecting EAS hadrons by means of thermal neutrons. The setup is located on the roofs of the experimental complex and the neighboring laboratory building; it includes six clusters of 12 detectors each. The total area of the installation is 1000 m^2 [10].

CALIBRATING NEVOD-EAS ENERGY, THRESHOLD, AND ANGULAR ACCURACY

To retrieve EAS parameters in a single event, we must know the absolute value of the energy released in each NEVOD-EAS detector station, which can be recalculated into the number of charged particles.

To calibrate NEVOD-EAS, response spectra are acquired every 4 h for all 36 detector stations in the self-triggering mode (i.e., charge signals are recorded from each station with no additional trigger conditions). These signals are mainly caused by single muons passing through a station. To a lesser extent, they can be caused by hadrons, high-energy electrons, and electrons from gamma-rays.

To calibrate the energy, a model of a detector station was developed in the Geant4 software package, which considers the detector's geometry and materials, along with the properties of the scintillator and photomultiplier. The response of a detector station to single muons, electrons, protons, and gamma rays was then modeled.

Close to actual differential spectra modeled in the CORSIKA software package for different values of zenith angles [11] were used in selecting the tracks of muons, protons, and gamma-quanta. To select the electron energy, we used a differential spectrum that combined results from CORSIKA modeling (for kinetic energies above 100 MeV) and calculations [12] for kinetic energies below 100 MeV.

Figure 1 shows experimental and modeled charge response spectra of a detector station in the self-triggering mode. The left peak in the experimental distribution is due to the contribution from beta-decay electrons and PMT dark noise. As can be seen from Fig. 1, the shapes of the experimental and model spectra agree in the region of detecting single particles, and the most probable charge is 27.5 pC. Results from Geant4 modeling allow us to determine that this charge corresponds to an energy release of 11.1 MeV inside a detector station. The ratio of the obtained values allows us to find the calibration coefficient used later in reconstructing experimental events: 0.40 MeV/pC.

To develop and debug ways of retrieving shower parameters, we modeled showers initiated by protons and iron nuclei in the 10^{14}–10^{17} eV range of primary

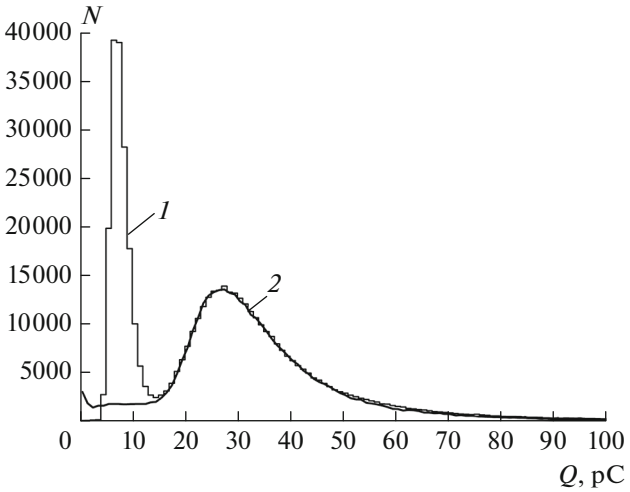

Fig. 1. Charge spectra of a NEVOD-EAS detector station response in the self-triggering mode: (*1*) experimental and (*2*) modeled.

energies and the 0°–50° range of zenith angles in the CORSIKA software package using the QGSJET-II-04 + FLUKA 2020.0.3 model of hadron interaction. The energy spectrum of primary particles had the power-law form with exponent $\gamma + 1 = 2.7$. The response of detector stations to shower particles was modeled using the Geant4 software package.

One of the most important parameters of the facility is the energy threshold. To estimate it, we analyzed the fraction of modeled events with axes near the center of the facility, for which at least seven clusters were operating with the maximum release of energy in the central cluster of the facility. A cluster is considered triggered if there are signals from at least two detector stations in it.

Figure 2 shows the energy spectra of all modeled showers initiated by protons and iron nuclei, along with showers that satisfy the conditions of selection. The spectra showed that 90% efficiency in recording proton-initiated showers was attained at an energy of 0.7 PeV. Proton showers with energies above 1 PeV were detected with an efficiency of more than 65%. For iron nuclei showers, a 50% efficiency of detection was attained at an energy of 1.4 PeV. At energies above 1 PeV, this figure was 46%. When near-vertical showers were selected (the range of zenith angles was 0° to 30°), the efficiency of detection was more than 98% at energies above 1 PeV for primary proton composition and more than 91% for showers from iron nuclei.

Joint analysis of events recorded by the NEVOD-EAS and DECOR facilities allowed a cross estimate of the accuracy of reconstructing the direction of a shower. The accuracy of reconstructing muon tracks in DECOR was better than 1°, so the angles of muon tracks in joint events can be considered a standard for

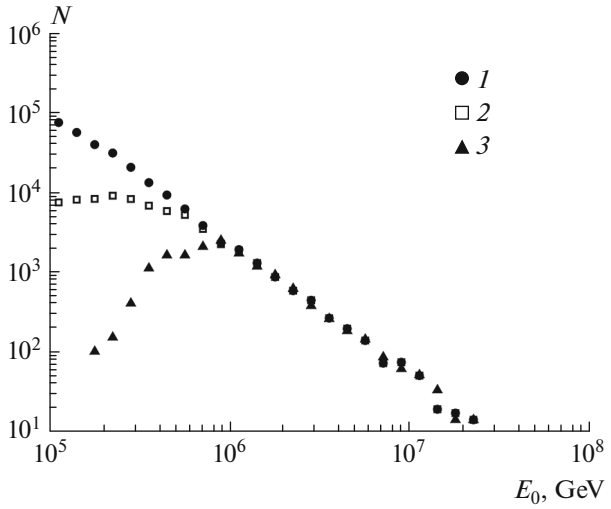

Fig. 2. Energy spectra: (*1*) spectrum of primary particles (protons and iron nuclei); (*2*) recorded spectrum of showers initiated by protons; (*3*) recorded spectrum of showers initiated by iron nuclei.

directions reconstructed from the NEVOD-EAS data. Only those DECOR events were selected for joint analysis, where at least three triggered supermodules and three quasi-parallel muon tracks were reconstructed. We selected 2456 joint events with a cluster triggering multiplicity of at least 5 over the period of exposure from July 1 to September 8, 2020.

Two techniques were used to reconstruct the direction of an EAS according to an analysis of NEVOD-EAS data. In the first of these, the direction was initially reconstructed from data of individual clusters, and the final vector of the EAS direction was the total vector from all clusters. The second way considered the data from all triggered stations as independent elements of the facility. A flat front approximation of an EAS was used in both approaches.

To estimate the accuracy of reconstructing the direction of an EAS, we determined the angle of divergence between the direction of a group of muons detected in DECOR and the direction of a shower reconstructed from NEVOD-EAS data. The distributions obtained for the angles of divergence are presented in Fig. 3. The 68th percentile of the event distribution was chosen as an estimate of the accuracy of recovery. The accuracy of reconstruction was thus $5.9° \pm 0.1°$ over individual clusters, and $3.5° \pm 0.1°$ over all detector stations.

As was shown in [7], reconstructing the directions of showers in modeled events using the first technique ensures an accuracy of better than 5° for primary particle energies above 1 PeV. The experimental results are thus in good agreement with the models.

STUDYING THE HADRON COMPONENT OF EASes

The detectors of the URAN facility are capable of detecting thermal neutrons that originate in interactions of hadrons in a shower's core with the matter surrounding the facility. Figure 4 shows the dependences of the number of neutrons detected by the URAN facility in experimental events on the EAS size [13] and the number of hadrons at the level of observation on a shower's size in modeled events (the same modeling as in the previous section).

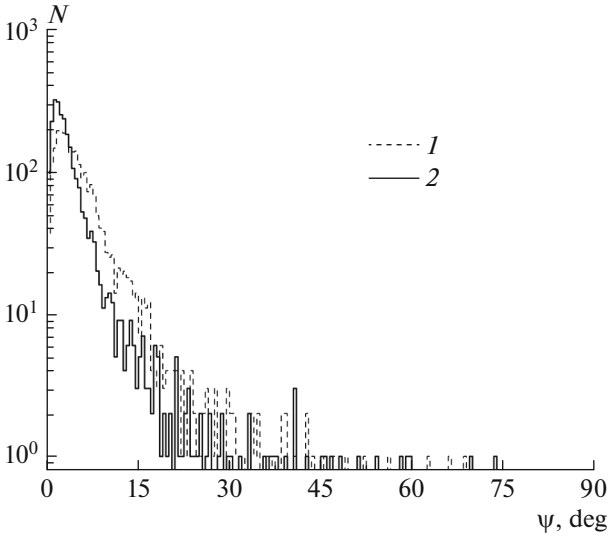

Fig. 3. Distributions over the angular deviations of EAS directions Ψ reconstructed according to NEVOD-EAS from the direction of muon tracks in the DECOR detector: (*1*) over all clusters; (*2*) over all detector stations.

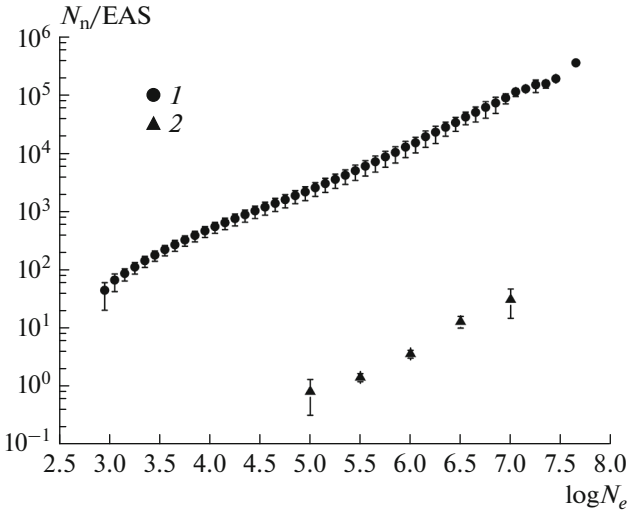

Fig. 4. Number of hadrons as a function of EAS size: (*1*) average number of hadrons at the level of observation, according to the QGSJET-II-04 + FLUKA 2020.0.3 model data; (*2*) average number of thermal neutrons detected in events by the URAN facility.

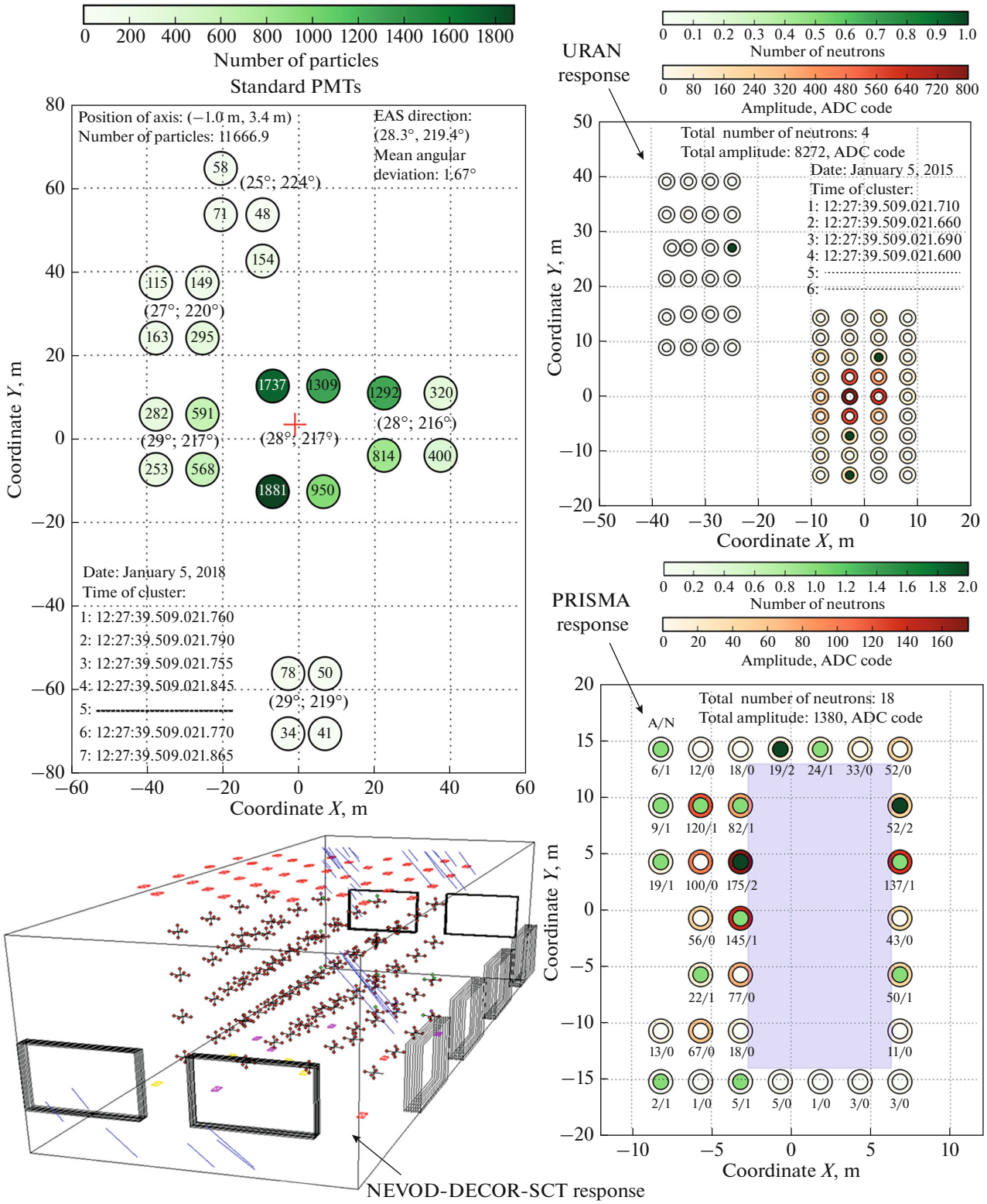

Fig. 5. Example of an event recorded by all facilities of the NEVOD Experimental Complex.

Both dependences are near linear on a double logarithmic scale, so the function is nearly power-law. The slope (exponent) for the experimental dependence is $\alpha = 0.89 \pm 0.09$; the exponent for modeled showers is $\alpha = 0.85 \pm 0.02$. These values coincide within the accepted error, so the number of thermal neutrons detected by the URAN facility is directly proportional to the number of hadrons in a shower.

The ratio of the dependences shown in Fig. 4 allowed us to estimate that the URAN facility detects an average of 1 thermal neutron per 3000 hadrons arriving at the level of observation. This property of the facility is planned to be used in verifying models of hadron–hadron interaction.

ANALYSIS OF MULTICOMPONENT EVENTS

All facilities of the NEVOD experimental complex were combined using a global time synchronization system that allows global time referencing of the events recorded by each facility with a temporal accuracy of 10 ns. A unified database has been developed for joint analysis of information from all facilities of the complex. Figure 5 shows an example of an event detected by the facilities of the experimental complex.

The top left part of the figure shows an event in the NEVOD-EAS facility (RUN 2018-01-05, the response time of the 3rd cluster is 12:27:39.509.021.755) reconstructed from data on the response of standard PMTs of detector stations. The bottom left part is a geometric reconstruction of responses of the NEVOD, DECOR, and SCT detectors in the same event (RUN 595, no. 514045, 12:27:39.509.022.094). The crosses show the triggered quasi-spherical optical modules of the Cherenkov water detector, the dots represent the triggered PMTs, and the rectangles indicate the triggered scintillation counters of the SCT. The right side of the figure shows the reconstructed responses of the URAN (top) and PRISMA (bottom) arrays, with their detectors indicated by concentric colored dots. The outer rings symbolize amplitude A of a counter's response to the EAS electromagnetic component (in ADC codes). The inner rings correspond to a counter's response during the detection of EAS neutrons (number N of detected neutrons). The corresponding color scales are shown for both facilities. For PRISMA, the amplitude and number of neutrons in each detector are additionally indicated by numbers in an A/N format. The cluster response times are given for URAN. The total number of neutrons detected and the amplitude of each response to the EAS electromagnetic component are given for both facilities.

According to the NEVOD-EAS data, the axis of a shower in this event was almost at the center of the Cherenkov water detector building where cluster no. 3 is located. This agrees with the distribution of particles of the electromagnetic component and neutrons in the detectors of the PRISMA and URAN facilities. The DECOR detector recorded 36 tracks of muons arriving at zenith and azimuth angles of 30° and 217°, respectively. This event at the NEVOD-EAS facility was characterized by the obtained direction of arrival with angles $\theta = 28°$ and $\varphi = 219°$.

This event is therefore an example of the simultaneous independent detection of the electron–photon, muon, and hadron components of an extensive air shower.

CONCLUSIONS

Modeling of the NEVOD-EAS setup shows that the most probable release of energy in a detector station in the self-triggering mode (the position of the muon peak) corresponds to 11.1 MeV, and the efficiency of detecting EASes with energies above 1 PeV is 65% for showers from protons and 46% for showers from iron nuclei. A comparison of the directions of particle in showers reconstructed from the NEVOD-EAS and DECOR data shows the difference to be less than 3.5° for 68% of the events. Cross analysis of experimental and modeled events confirm that the number of thermal neutrons detected by the URAN facility was directly proportional to the number of hadrons in a shower. The NEVOD Experimental Complex thus allows us to study the electron–photon, muon, and hadron components of extensive air showers simultaneously.

FUNDING

This work was supported by the Russian Science Foundation, project no. 22-72-10010.

REFERENCES

1. Prosin, V.V., Astapov, I.I., Bezyazeekov, P.A., et al., *Bull. Russ. Acad. Sci.: Phys.*, 2021, vol. 85, no. 4, p. 395.
2. Shchegolev, O.B., Alekseenko, V.V., Kuleshov, D.A., et al., *Bull. Russ. Acad. Sci.: Phys.*, 2021, vol. 85, no. 4, p. 415.
3. Yashin, I.I., Amelchakov, M.B., Astapov, I.I., et al., *J. Instrum.*, 2021, vol. 16, p. T08014.
4. Kindin, V.V., Amelchakov, M.B., Barbashina, N.S., et al., *Instrum. Exp. Tech.*, 2018, vol. 61, no. 5, p. 649.
5. Amelchakov, M.B., Bogdanov, A.G., Zadeba, E.A., et al., *Instrum. Exp. Tech.*, 2018, vol. 61, no. 5, p. 673.
6. Barbashina, N.S., Ezubchenko, A.A., Kokoulin, R.P., et al., *Instrum. Exp. Tech.*, 2000, vol. 43, no. 6, p. 743.
7. Amelchakov, M.B., Barbashina, N.S., Bogdanov, A.G., et al., *Nucl. Instrum. Methods Phys. Res., Sect. A*, 2022, vol. 1026, p. 166184.
8. Gromushkin, D.M., Alekseenko, V.V., Petrukhin, A.A., et al., *J. Instrum.*, 2014, vol. 9, no. 8, p. C08028.
9. Gromushkin, D.M., Volchenko, V.I., Zadeba, E.A., et al., *Bull. Russ. Acad. Sci.: Phys.*, 2015, vol. 79, no. 3, p. 380.
10. Gromushkin, D.M., Bogdanov, F.A., Khokhlov, S.S., et al., *J. Instrum.*, 2017, vol. 12, no. 7, C07029.
11. Kovylyaeva, A.A., Dmitrieva, A.N., Tolkacheva, N.V., and Yakovleva, E.I., *J. Phys.: Conf. Ser.*, 2013, vol. 409, p. 012128.
12. Daniel, R.R. and Stephens, S.A., *Rev. Geophys. Space Phys.*, 1974, vol. 12, no. 2, p. 233.
13. Bogdanov, F.A., Gromushkin, D.M., Izhbulyakova, Z.T., et al., *Bull. Russ. Acad. Sci.: Phys.*, 2021, vol. 85, no. 4, p. 424.

Translated by O. Ponomareva